Journal of Solid State Chemistry 183 (2010) 696–701

Contents lists available at ScienceDirect

Journal of Solid State Chemistry

journal homepage: www.elsevier.com/locate/jssc

# Triple assembly of ZnO, large-scale hollow spherical shells with flower-like species consisting of rods grown on the outer surfaces of shells

Yazhuo Shang, Jun Hu, Honglai Liu *, Ying Hu

*Key Laboratory for Advanced Materials, East China University of Science and Technology, Shanghai, 200237, China*

ARTICLE INFO

*Article history:*
Received 7 October 2009
Received in revised form
5 January 2010
Accepted 9 January 2010
Available online 20 January 2010

*Keywords:*
Ionic liquids
Large-scale hollow shell
Flower like
Rod

ABSTRACT

Novel large-scale hollow ZnO spherical shells were synthesized by ionic liquids assisted hydrothermal oxidization of pure zinc powder without any catalyst at a relatively low temperature of 160 °C. X-ray diffraction (XRD), energy dispersive X-ray spectroscopy (EDX) and scanning electron microscopy (SEM) patterns show that the shells are composed of ZnO and the structure of the shells is very unique. Textured flower-like ZnO consisting of ZnO rods is grown on the outer surfaces of shells forming a triple assembly. Room-temperature photoluminescence spectra of the oxidized material show a sharp peak at 379 nm and a wider broad peak centered at 498 nm. The possible growth mechanism of the triple assembly of ZnO is discussed in detail.



## 1. Introduction

Zinc oxide (ZnO) is a versatile smart material that has key applications in catalysts, sensors, piezoelectric transducers, transparent conductors, solar cells, field-emission displays, and surface acoustic wave devices because of its wide band gap (3.2 eV) with low lasing threshold, higher exciton binding energy (60 meV), higher optical gain than other semi-conductor as well as the potential for nanoscale electronic and optoelectronic devices [1–4]. In the past few years, ZnO nanomaterials with one-dimensional (1-D) structure such as nanobelts, nanobridges, nanonails, nanoribbons, nanowires, and nanorods have been widely studied [5–8]. Correspondingly, numerous approaches including thermal evaporation of oxide powders, the calcination method, hydrothermal and solvothermal process were reported. Recently, large-scale (nanometer or submicrometer) three-dimensional hollow ZnO materials have attracted increasing interest because of their unique structure, interesting properties that differ from their solid counterparts, and widespread applications in drug delivery, catalysts, photonic crystals, nanoreactors, etc. The synthesis of individual ZnO superstructure with hollow interiors would enable their use as building blocks for new photonic crystals and other model systems for light scattering, which are of fundamental importance to both theoretical and experimental sciences [9]. Mesoporous polyhedral cages and shells formed by textured self-assembly of ZnO nanocrystals were synthesized by Gao and Wang [10]. Jiang et al. [11] prepared polyhedral submicrometer-sized hollow beads of single-crystalline ZnO using laser-assisted growth with ethanol droplets as soft templates. ZnO hollow shells were synthesized by thermal evaporation of Zn at 500 °C in a tube furnace under the flow of argon and oxygen gas mixture [12]. Lu et al. [13] successfully fabricated hollow ZnO microstructures and ZnO microberets by simple thermal evaporation of pure zinc powder. Khan adopted a simple route to realize the growth of large scale metallic Zn microspheres and hollow ZnO microspheres [14]. Gas bubble soft-template methods [15,16] also can be used in synthesis of hollow ZnO microspheres. It can be mentioned that with the development of science and technology, ionic liquids also were introduced into the synthesis of ZnO. Dai and Taubert have reported extensively on the formation of ZnO from ionic liquids [17,18]. Very recently, zinc oxide particles with unusual nanostructures: hollow ZnO rods, flower-like ZnO particles, porous ZnO microspheres as well as aligned ZnO arrays with branched rods, hexagonal rods, quasi-round rods, hexagonal pyramids and porous nanostructures have been constructed in ionic liquid aqueous solution by Li et al. [19–21]. These results not only provide feasible ways to assemble building blocks for future functional devices but also offer opportunities to explore their potential properties. However, self-organization of one-dimensional (1-D) ZnO into three-dimensional (3-D) hollow shells or spheres is still challenging, further work is still needed to explore the path of making hollow materials and to understand their growth process.

We report here a remarkable large scale self-assembled shell formed by triple assembly of ZnO, which is made by a novel ionic

* Corresponding author. Fax: +86 21 64252921.
*E-mail address:* yazhuoshang@ecust.edu.cn (H. Liu).

0022-4596/$ - see front matter © 2010 Elsevier Inc. All rights reserved.
doi:10.1016/j.jssc.2010.01.009

liquids-assisted hydrothermal oxidization of pure zinc powder without any catalyst at a relatively low temperature of 160 °C. The shells exhibit unique morphologies, and their walls are composed of textured flower-like ZnO consisting of ZnO rods. The structures of the shells are studied, and a possible growth mechanism is proposed. Compared to the other synthetic methods, this method is notably simple, convenient and inexpensive. We believe that these large-scale crystalline ZnO hollow shells, a new member of the ZnO structure family, should find new applications and the as-developed route will be helpful in the future fabrication of both ZnO and other semi-conductor materials with micro- and nano-sized structures in an easy and inexpensive way.

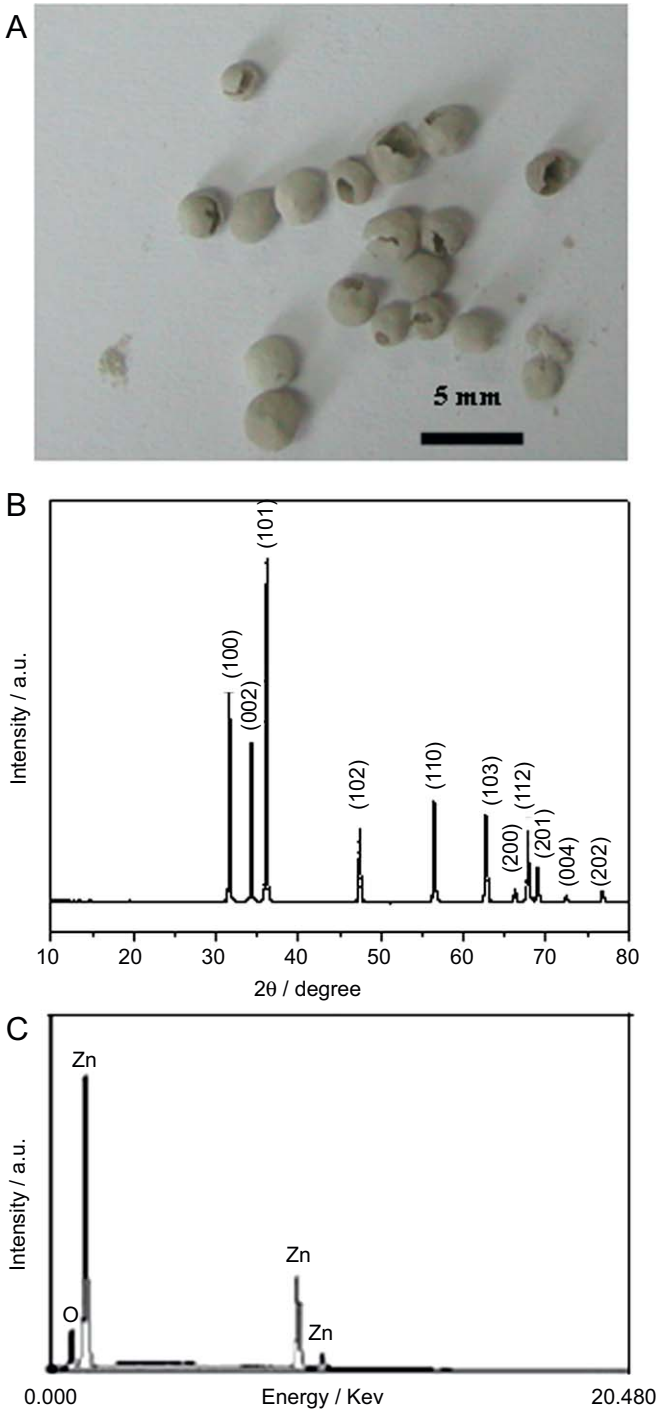


**Fig. 1.** Macroimage (A), XRD pattern (B) and EDX spectrum (C) of the hollow ZnO shells.

## 2. Experimental section

The hollow ZnO microstructures are usually grown by solid–vapor deposition process and e-beam sputtering. The structures in this work were synthesized by a novel ionic liquids-assisted hydrothermal oxidization of pure zinc powder without any catalyst at a relatively low temperature of 160 °C. A typical experimental procedure is as follows: 1.2 g of zinc powder (analytical grade, purchased from Shanghai Aijian Reagent Co., Ltd. and used without further treatment, the average size of the zinc powder used in this work is about 10 μm in diameter) was

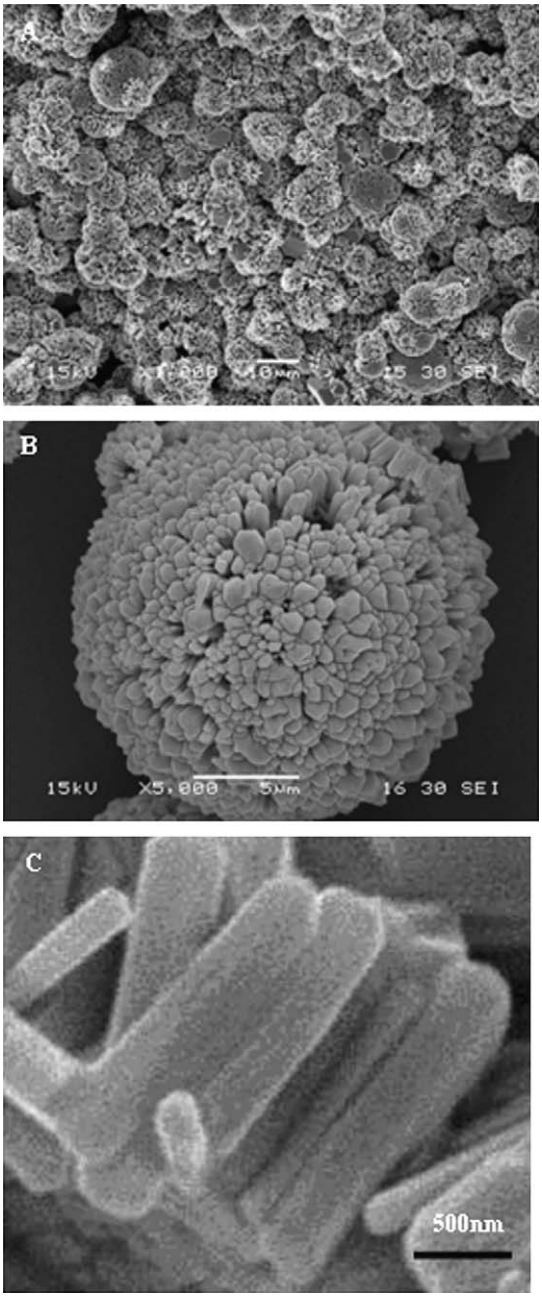


**Fig. 2.** Low-magnification SEM image showing the flower like ZnO outside the shell structure (A), SEM image of the ZnO flower (B), SEM image of ZnO rods that are composed of flowers (C).

introduced into 40 mL aqueous solution of ionic liquids (1-octyl-3-methylimidazolium bromide, the concentration is 0.4 mol/L) under ultrasonic treatment. The grey mixture was then transferred into teflonlined stainless steel autoclaves with a size of 50 ml, sealed, and maintained at 160 °C. After being aged for 5 h the resulting solid products were repeatedly washed with deionized water and ethanol to remove the ionic liquids. The final products were collected and dried at 50 °C in air.

The as-prepared products were characterized and analyzed by X-ray diffraction (XRD) (D/Max2550 VB/PC diffractometer with Cu Ka radiation). The scanning electron microscopy (SEM, equipped with EDX) images were obtained on JSM-T20. The macroimage of the products was taken by Olympus Digital Camera (C-4040ZOOM, Made in Japan). The photoluminescence (PL) spectra were measured using a Xe laser as the excitation source (350 nm).

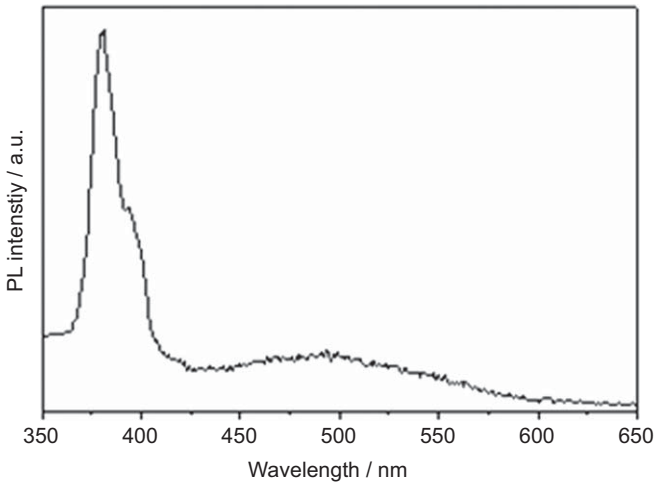


**Fig. 3.** Photoluminescence spectrum of hollow ZnO spherical shells.

## 3. Results and discussions

The image of ZnO products obtained at 160 °C for 5 h taken by olympus digital camera is shown in Fig. 1A. The image shows that the as-obtained ZnO products are composed of uniform, hollow spherical architectures ranging from 2 to 3 mm in diameter. The phase purity of the products examined by XRD is depicted in Fig. 1B. All diffraction peaks can be indexed to the pure hexagonal wurtzite phase of ZnO (JCPDS card no. 36-1451) with lattice constants $a$=3.249 Å and $c$=5.206 Å. No peaks from any other phase of ZnO and impurities are observed. The as-prepared samples possess higher crystallinity as is evident from the diffractogram where all peaks have higher and narrower shapes. The EDX spectrum (Fig. 1C) also reveals that the atomic ratio of Zn/O is nearly 1:1, which is consistent with the stoichiometric ZnO. It is obvious that the samples in this work are composed of ZnO with a pure hexagonal wurtzite structure.

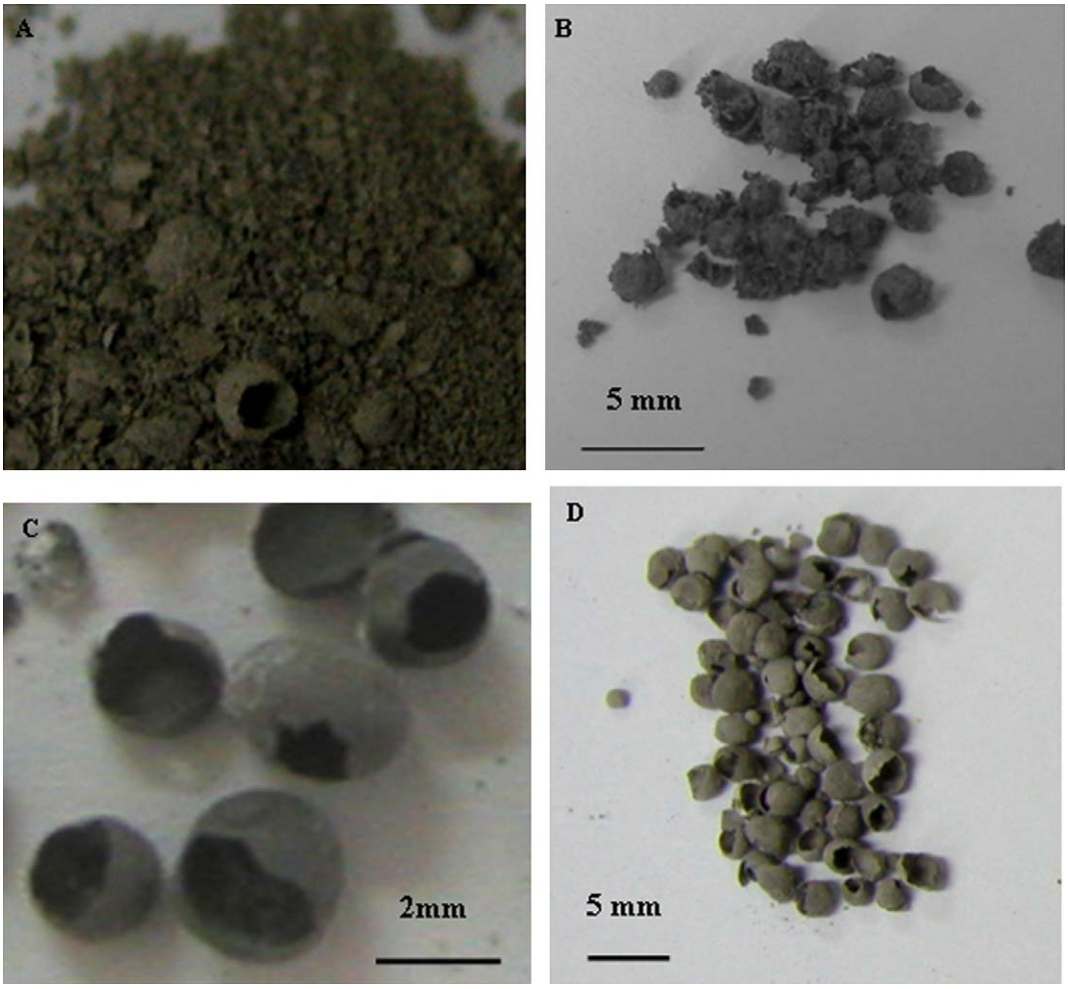


**Fig. 4.** The morphology of products of different reaction times: (A) 1 h; (B) 1.5 h; (C) 2 h; (D) 3 h.

The microstructures of the products further characterized by SEM are displayed in Fig. 2. The typical low-magnification SEM image provides the surface morphology of the macro-shell structure (Fig. 2A). As shown from the image, the shells are constructed by many ZnO flowers with an average diameter of 10 μm (Fig. 2B). Further observation indicates that the single ZnO flower is composed of small ZnO rods with diameters of 200–300 nm (Fig. 2C).

The PL spectra were measured to study the optical properties of hollow ZnO spherical shells. The experiments were conducted with excitation photon energy (350 nm Xe laser) greater than that of ZnO band gap at room temperature. Fig. 3 shows the room-temperature PL spectrum, which consists of two emission bands: a strong UV emission at 379 nm and a weak broad green emission centered at around 498 nm, respectively. The UV emission peak of ZnO is generally attributed to the near-band-edge emission of the wide band gap of ZnO due to the excitonic recombination [22], and the green emission band is typically thought to be related to the single ionized oxygen vacancy coming from the recombination of a photon-generated hole with the single ionized charged state of the defect in ZnO [23]. Moreover, it was reported that the oxygen vacancies responsible for the green emission are located at the surface [24]. The presence of UV emission at room temperature indicates that the as-prepared material is indeed ZnO and may be polycrystalline. It is likely that green emission in ZnO shells mainly originates from surface defects. The as-prepared samples possess such a high crystallinity that the point defect density in ZnO flowers attached to ZnO shells is low. Therefore, the green emission derived from surface defects appears very weak. Certainly, the weak green emission band can also be attributed to the strict stochiometric composition of the as-prepared ZnO [25,26], which coincides with the EDX result. The PL results recorded for the hollow ZnO spheres indicate that the simple hydrothermal process of the zinc powder produces hollow ZnO microspheres with all features characterizing its bulk counterpart retained.

In order to explore the growth behavior of large-scale shells, we examine the intermediate products obtained at different times during the experimentation. The morphologies of products at different reaction times are shown in Fig. 4. The obtained species were also further observed and analyzed by SEM and XRD. The XRD patterns show that all the products are a mixture of ZnO and Zn. These results provide the necessary information for developing a model of the formation of ZnO shells. It can be mentioned that the formation of flowers outside the shells is far behind the formation of shell itself through analyzing the SEM image. The SEM image shown in Fig. 5A gives a detailed morphology of the black shells (in Fig. 4C). It can be seen that the shells are accumulated by small spherical particles densely. XRD pattern (Fig. 5B) reveals that the shells are a mixture of ZnO and Zn. Obviously, shortening the reaction time makes the reaction remain uncompleted, the shells composed of spherical particles were formed before the formation of flowers and these particles are the rudiments of ZnO flowers.

Based on the above characterizations and description, the growth mechanism is discussed in detail as follows, and the corresponding schematic illustrations of the formation process are shown in Fig. 6.

In the hydrothermal reaction system, the chemical reactions to form ZnO are formulated as follows:

$$Zn + H_2O \rightarrow Zn^{2+} + OH^- + H_2\uparrow \quad (1)$$

$$Zn^{2+} + OH^- \leftrightarrow \begin{cases} Zn(OH)_2 \\ Zn(OH)_4^{2-} \end{cases} \quad (2)$$

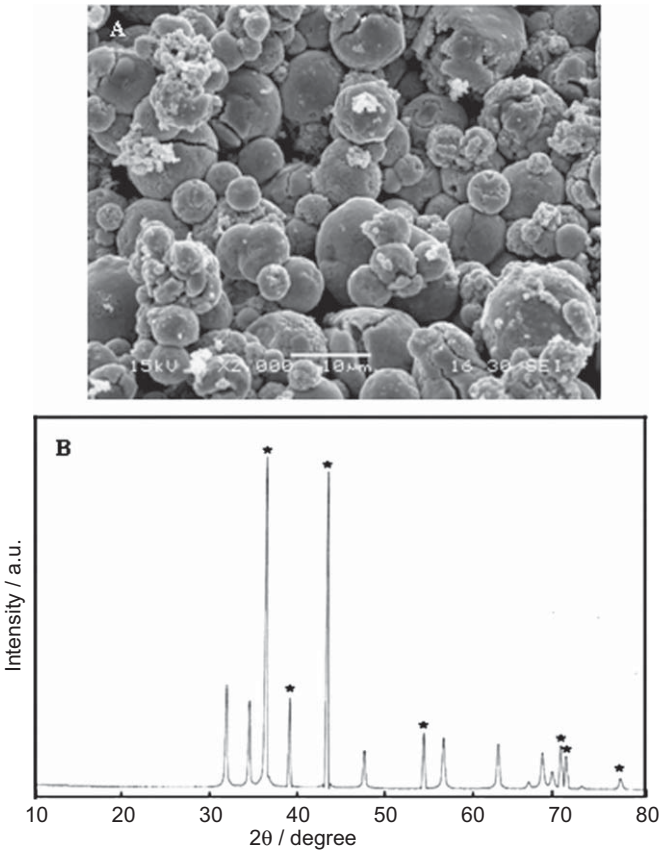


**Fig. 5.** SEM image (A) and XRD pattern (B) of the hollow shells (in Fig. 4C). (* reflections of zinc)

$$Zn(OH)_2 \rightarrow ZnO + H_2O \quad (3)$$

As illustrated in Fig. 6, during the hydrothermal process the microcavity in zinc powder will expand and at the same time, many microbubbles of $H_2$ are produced in reaction 1 with increase in temperature. The existence of gases provides the aggregation center for surface active materials, namely, ionic liquids. The molecules of ionic liquids tend to aggregate on the gas–liquid interface between gas and water that strengthen the membrane of bubbles dramatically because of the hydrophobic interaction and hydrogen bonds among ionic liquids and water molecules. The microstructure of microbubbles is shown in Fig. 6A. The microbubbles with elastic membranes are the rudiments of the final shells (step A). Driven by the minimization of interfacial energy, small Zn particles may aggregate around the bubbles interface to form hollow Zn particle-dotted shells (step B). The microstructure of this species is shown in Fig. 6B. With the process of reaction 1, parts of the newly produced $H_2$ penetrate into the bubble, leading to its accretion. In a stepwise manner, the Zn particle-dotted bubble goes upward until reaching the aqueous surface (step C). This may be the reason why the samples always stick on the lid of the autoclave. It is worth mentioning that during these courses, the aggregation of small Zn particles on the interface of bubbles and the chemical reaction are continuing, the shell outside the bubble will become harder and harder; correspondingly, it will become bigger and bigger until the shell is hard enough and cannot be enlarged.

With regard to the origin of the sphere gaps, Gao and Wang [10] attributed to the Zn–ZnO lattice mismatch, the Zn inside sublimates through the gaps because of its relatively lower melting point than that of ZnO. In our case, perhaps the lattice mismatch is not the main cause; the inner vapor pressure of shells

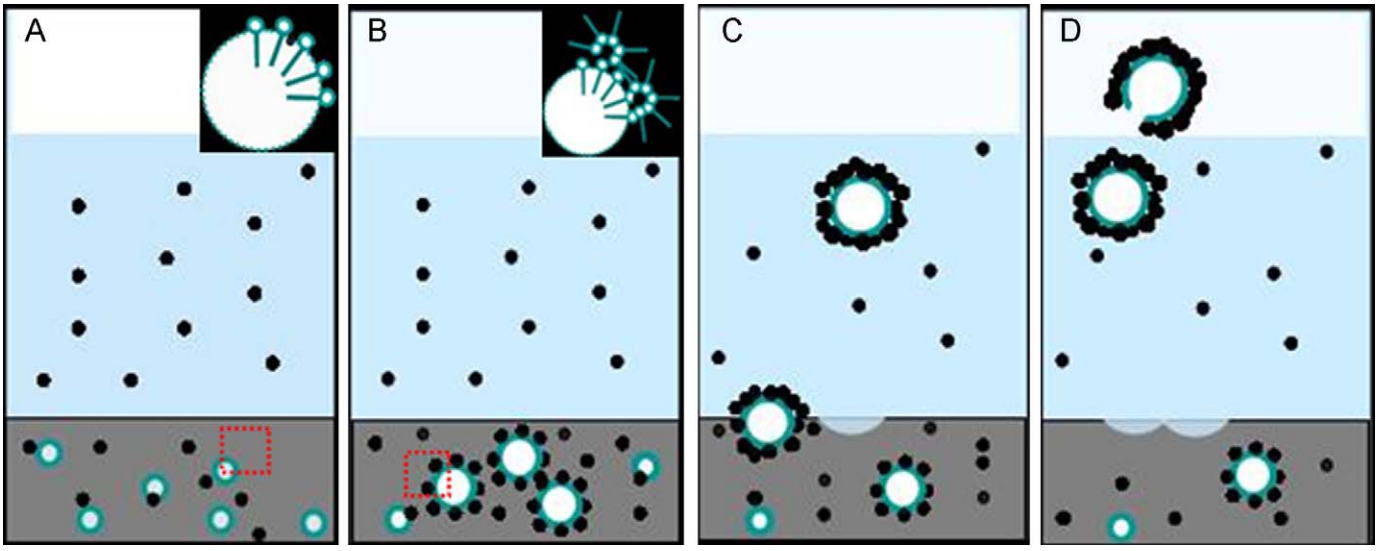


**Fig. 6.** A proposed growth mechanism for the formation of large scale shells: (A) formation of bubbles; (B) formation of shells; (C) floatage of shells; (D) the breach of shells.

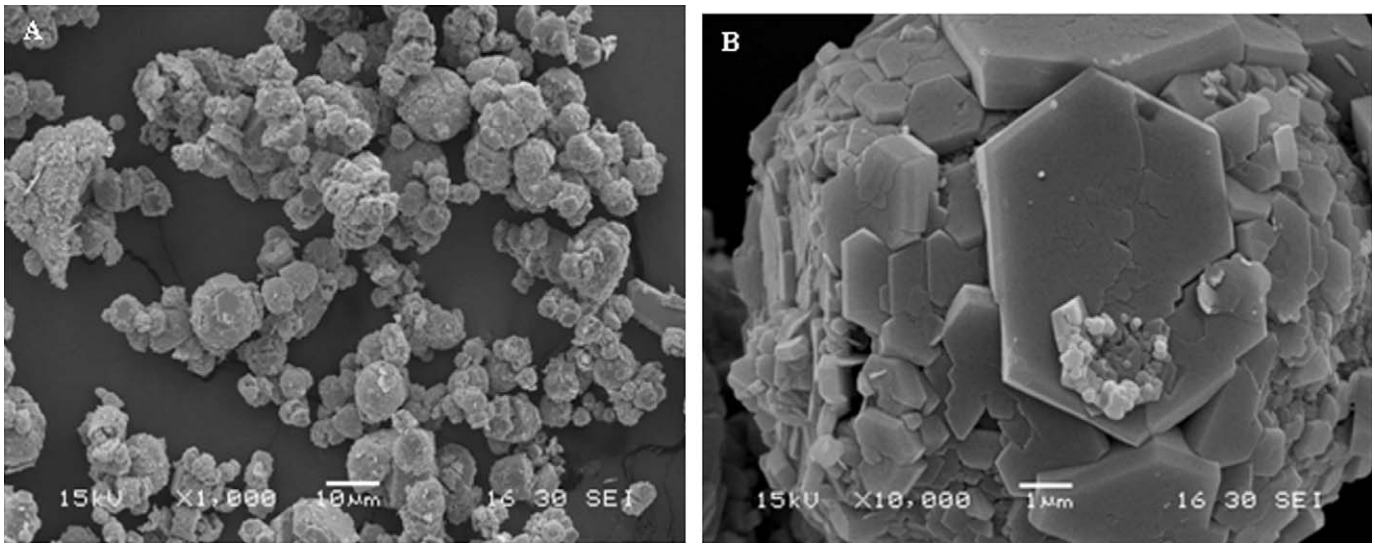


**Fig. 7.** SEM image of ZnO prepared by hydrothermal process without ionic liquids assisted (A) and an individual spherite (B).

is predominant. The shell is breached when the inner vapor pressure becomes greater than what the local shell can sustain (step D). The particles forming the shells will evolve into ZnO flowers constructing of rods is probably similar to the formation of flower-like ZnO by Gemini surfactant-assisted hydrothermal process that has been explained in detail in our previous work [27].

To illuminate the role of the ionic liquids in the self-assembly of ZnO rods into large scale hollow shells, the products obtained via the hydrothermal reaction without ionic liquids were characterized. We cannot see the large-scale hollow shells by the naked eye and the SEM results are shown in Fig. 7. SEM observation indicates that the as-synthesized spherical ZnO with diameters of 5–10 μm is scattered, and do not further assemble into a superstructure. The spherites are composed of numerous sheet-like particles and most of the sheets are hexagonal. It reveals that ionic liquids play an important role in the formation of hollow shells constructed with ZnO rods.

Ionic liquids have special physico-chemical characteristics such as the low melting point, extremely low vapor pressure, favorable salvation behavior, and high reactivity and selectivity. They have been widely studied in the past decade [28–37]. The study on the surface active characteristic of ionic liquids has proved that ionic liquids with long hydrophobic substituent alkyl groups on the cation behave as surfactants. The cmc values of ionic liquids (CnmimBr) in aqueous solution are lower than those of the traditional surfactant alkyltrimethylammonium bromides (CnTAB) with the same alkyl tail [38]. The excellent surface active properties enable the molecules of ionic liquids to aggregate on the surface of bubbles at the beginning of a period of time in the hydrothermal process, which strengthens the membrane of bubbles dramatically. These membranes are much more stable and elastic even at high temperature (below 300 °C) compared with that composed by traditional surfactants because of the higher thermal stability of ionic liquids and the extra hydrogen bonds among ionic liquids and water molecules. During the formation of ZnO flower composed by rods, the molecules of ionic liquids act as not only the stabilizer, structure directing agent but also growth units ($Zn(OH)_4^{2-}$) carrier just as Gemini surfactants do [27].

Moreover, the reaction time, the concentration and the kind of ionic liquids, as well as the pre-reserved space of autoclaves before seal are all parameters that influence the shell structures. The corresponding work is in progress.

## 4. Conclusions

We have reported a new structure, a large-scale hollow ZnO spherical shell, which is made by a novel triple-assembly process during hydrothermal process assisted by ionic liquids. The shells exhibit unique microstructure, and their walls are composed of textured ZnO flowers consisting of ZnO rods. The possible growth mechanism of hollow ZnO spherical shells is proposed, which is composed of the formation of bubbles, the formation of particle-dotted bubble, floatage, breach of Zn/ZnO shells as well as the formation of flowers. We believe this unique morphology of ZnO may make it attractive to be used in many fields and the as-developed method is simple, convenient and inexpensive, that will be helpful in the future fabrication of both ZnO and other semi-conductor materials with macro-, micro- and nano-sized structures.

## Acknowledgments

This work was supported by the National Natural Science Foundation of China (Projects no. 20706013, 20736002), Program for Changjiang Scholars and Innovative Research Team in University (no. IRT0721) and the 111 Project of Ministry of Education of China (no. B08021).

## References

[1] E. Wong, P. Searson, Appl. Phys. Lett. 74 (1999) 2939–2941.
[2] S. Choopum, R. Vispute, W. Noch, A. Balsamo, R. Sharma, T. Venkatesan, Appl. Phys. Lett. 75 (1999) 3947–3949.
[3] J. Zhang, L. Sun, H. Pan, C. Liao, C. Yan, New J. Chem. 26 (2002) 33–35.
[4] H. Zhang, D. Yang, Y. Ji, X. Ma, J. Xu, D. Que, J. Phys. Chem. B 108 (2004) 3955–3958.
[5] K. Yang, Z. Wang, Nano Lett. 12 (2003) 1625–1631.
[6] J. Lao, J. Huang, D. Wang, Z. Ren, Nano Lett. 3 (2003) 235–238.
[7] C. Ye, G. Meng, Y. Wang, Z. Jiang, L. Zhang, J. Phys.Chem. B 106 (2002) 10338–10341.
[8] M. Huang, Y. Wu, H. Feick, N. Tran, E. Weber, P. Yang, Adv. Mater. 13 (2001) 113–116.
[9] X. Sun, Y. Li, Angew. Chem. 43 (2004) 3827–3831.
[10] P. Gao, Z. Wang, J. Am. Chem. Soc. 125 (2003) 11299–11305.
[11] Z. Jiang, Z. Xie, X. Zhang, S. Lin, T. Xu, Adv. Mater. 16 (2004) 904–907.
[12] Y. Leung, K. Tam, A. Djurisic, M. Xie, J. Cryst. Growth 283 (2005) 134–140.
[13] H. Lu, L. Liao, J. Li, D. Wang, Hui. He, Q. Fu, Lei. Xu, Yu. Tian, J. Phys. Chem. B 110 (2006) 23211–23214.
[14] K. Aurangzeb, M. Wojciech, E. Martin, Physica E 33 (2006) 331–335.
[15] C. Yan, D. Xue, F. J. Alloys Compd. 431 (2007) 241–245.
[16] L. Li, H. Yang, G. Qi, J. Ma, X. Xie, H. Zhao, F. Gao, Chem. Phys. Lett. 455 (2008) 93–97.
[17] H. Zhu, J. Huang, Z. Pan, S. Dai, Chem. Mater. 18 (2006) 4473–4477.
[18] Z. Li, P. Rabu, P. Strauch, A. Mantion, A. Taubert, Chem.—Eur. J. 14 (2008) 8409–8417.
[19] Z. Li, Y. Luan, T. Mu, G. Chen, Chem. Commun. 10 (2009) 1258–1260.
[20] Z. Li, Y. Luan, Q. Wang, G. Zhuang, Y. Qi, Y. Wang, C. Wang, Chem. Commun. 41 (2009) 6273–6275.
[21] Z. Li, Q. Yu, Y. Luan, CrystEngComm 12 (2009) 2683–2687.
[22] Y. Kong, D. Yu, B. Zhang, W. Fang, S. Feng, Appl. Phys. Lett. 78 (2001) 407–409.
[23] K. Vanheusdan, W.L. Warren, C.H. Seager, D.R. Tallent, J.A. Voigt, B.E. Gnade, J. Appl. Phys. 79 (1996) 7983–7986.
[24] D. Li, Y. Leung, A. Djurisic, Z. Liu, M. Xei, S. Shi, S. Xu, W. Chan, Appl. Phys. Lett. 85 (2004) 1601–1603.
[25] U. Ozgur, Y. Alivov, C. Liu, A. Teke, M. Reshchikov, S. Dog-brevean, V. Avrutin, S. Cho, H. Morkoc, J. Appl. Phys. (2005) 041301.
[26] K. Vanheusden, W.L. Warren, C.H. Sesger, D.R. Tallant, J.A. Voigt, B.E. Gnage, J. Appl. Phys. 79 (1996) 7983–7987.
[27] Y. Shang, H. Liu, J. Xia, Z. Xu, J. Disp. Sci. Technol. 26 (2005) 525–530.
[28] A. Heintz, J. Chem. Thermodyn. 37 (2005) 525–535.
[29] R. Vany′ur, L. Bicz′ok, Z. Miskolczy, Colloids Surf. A 299 (2007) 256–261.
[30] J. Wang, H. Wang, S. Zhang, H. Zhang, Y. Zhao, J. Phys. Chem. B 111 (2007) 6181–6188.
[31] Y. Gao, S. Han, B. Han, G. Li, D. Shen, H. Li, J. Du, W. Hou, G. Zhang, Langmuir 21 (2005) 5681–5684.
[32] B. Dong, N. Li, L. Zheng, L. Yu, Langmuir 23 (2007) 4178–4182.
[33] Z. Li, Z. Jia, Y. Luan, T. Mu, Curr. Opin. Solid State Mater. Sci. 12 (2009) 1–8.
[34] R. Gobel, A. Friedrich, A. Taubert, Dalton Trans. 39 (2010) 603–611.
[35] Z. Li, A. Taubert, Molecules 14 (2009) 4682–4688.
[36] A. Taubert, I. Arbell, A. Mecke, Gold Bull. 39 (2006) 205–211.
[37] A. Taubert, Acta Chim. Slovenica 52 (2005) 183–186.
[38] R. Vany′ur, L. Bicz′ok, Z. Miskolczy, Colloids Surf. A 299 (2007) 256–261.